JOURNAL OF THERMOPHYSICS AND HEAT TRANSFER
Vol. 6, No. 2, April–June 1992

# Numerical Solutions of Natural Convection in Enclosure with Boundary Condition Switching Method

Z. Fang* and I. Paraschivoiu†
*Ecole Polytechnique de Montréal, Montréal, Quebec H3C 3A7, Canada*

**Numerical solutions of the natural convection equations with FEM and FDM have been applied to study the convection heat transfer in square cavities and vertical annuli with high-aspect ratio. The boundary condition switching method is employed to solve the Navier-Stokes equations with primitive variables. On boundaries where both Dirichlet and Neumann boundary conditions are known, the Neumann boundary condition is satisfied naturally whereas the Dirichlet boundary condition is switched to substitute the unknown boundary condition of the other variable; for instance, vorticity in stream function-vorticity equations, and pressure in Navier-Stokes equations. With the boundary condition switching, equal order interpolation in FEM and nonstaggered grid in FDM can be used without upwinding formulation. The present scheme is tested by both finite element method and finite difference method for convection heat transfer in square cavities and applied to convection heat transfer in vertical annuli.**

## Nomenclature

$A$ = aspect ratio
$k$ = thermal conductivity
$M$ = stiffness matrix
$N$ = element shape function
$n$ = normal vector
$P$ = pressure
$Pr$ = Prandtl number
$Ra$ = Rayleigh number
$T$ = temperature
$u, v$ = velocity components
$V$ = velocity vector
$W$ = weighting function
$\alpha$ = thermal diffusivity
$\beta$ = thermal expansion coefficient
$\Gamma$ = boundary of domain
$\nu$ = kinematic viscosity
$\rho$ = density
$\Omega$ = domain

## Introduction

NATURAL convection in enclosures has been given extensive consideration in the literature. This kind of heat transfer problem has gained broad interest and application. Natural convection heat transfer in vertical annuli falls into this category. It finds applications in areas such as reactor cooling and furnace design. In the present work, convection heat transfer in vertical annuli with high-aspect ratio is simulated numerically. The physical geometry consideration is that the inner wall is maintained at constant heat flux and the outer wall is kept at a constant temperature with the top and bottom of the annulus insulated. In the literature, only a few studies for this geometry can be found. One of the earlier experimental studies for this physical geometry was provided by Sheriff.[1] In his work, more attention was paid to low diameter ratio. Keyhani et al.[2] and Bhushan et al.[3] studied the convection heat transfer in the same physical geometry for diameter ratios much higher than unity. Earlier numerical studies for similar cases were done by de Vahl Davis and Thomas.[4,5] In their work, the inner wall temperature was also kept at a constant temperature. Numerical studies for vertical annuli with a constant heat flux at the inner wall and a constant temperature at the outer wall were done by Khan and Kumar[6] for a range of diameter ratios and up to medium aspect ratios. In this work, convection heat transfer in vertical annuli with high-aspect ratio is studied. Results are obtained by solving the Navier-Stokes equations by both FEM and FDM methods.

In the present work, the boundary condition switching method introduced by Peeters et al.[7] to solve the stream function-vorticity equations for incompressible laminar flows is applied to solve the Navier-Stokes equations with primitive variables. Previous methods for solving stream function-vorticity equations include iterative updating of the vorticity boundary conditions.[8–12] The no-slip boundary condition at the wall boundary is implemented through evaluation formulae for the vorticity boundary condition at the walls. With the boundary condition switching method, the no-slip solid wall boundary condition is applied by taking the advantage of implementation of the natural Neumann boundary condition. The no-penetration boundary condition is switched to substitute the vorticity boundary condition, eliminating the need for an iterative evaluation of wall vorticity formulae. This method has been applied to solve compressible flow problems by Habashi et al.[13]

When solving the Navier-Stokes equations with primitive variables for incompressible laminar flows, situations exist where both Dirichlet and Neumann boundary conditions are known. On wall boundaries the Dirichlet boundary condition is zero velocity. The natural Neumann boundary conditions are given by continuum theory. Traditional methods to solve Navier-Stokes equations with primitive variables are to implement the velocity boundary conditions with the natural boundary condition satisfied by the continuity equation. It is well known that this method results in pressure oscillations using equal order interpolation in the finite element method[14] and using a nonstaggered grid in the finite difference method.[15] This difficulty can be removed by using the boundary condition switching method. The natural boundary condition required by the continuum theory is satisfied naturally as in the no-slip boundary condition in stream function-vorticity equations. The related velocity boundary condition can be switched to replace the continuity equation on wall boundary. In this way, the velocity boundary conditions and the natural Neu-

Received Oct. 23, 1990; revision received May 20, 1991; accepted for publication May 22, 1991. 

*Research Associate, Department of Mechanical Engineering. Member AIAA.
†J.-A. Bombardier Aeronautical Chair Professor, Department of Mechanical Engineering. Member AIAA.

mann boundary condition are implemented explicity with the continuity equation satisfied.

In this work, both the finite element weighted residual formulation and the finite difference method are employed to solve convection heat transfer problems within enclosures. In the finite element method, equal order interpolation for both velocity and pressure is used; in the finite difference method, a nonstaggered grid is used. Computational results show that, with the boundary condition switching method, there are no pressure oscillations in the numerical solutions. Thus, pressure solutions do not need to be filtered or smoothed. First, the solution procedure is applied to solve the convection heat transfer in a square cavity. In order to verify the solution procedure, numerical results are compared with solutions in the literature.[16,17] Then, convection heat transfer in vertical annuli with high-aspect ratio is studied by applying the boundary condition switching scheme. Numerical results are compared with experimental data.

## Boundary Condition Switching Technique

The boundary condition switching scheme to solve the Navier-Stokes equations with primitive variables is based on boundary condition analysis. Two-dimensional steady incompressible laminar flows in Cartesian grid are chosen to illustrate this method. The governing equations are the continuity equation and the momentum equations. These equations are

$$V\cdot\nabla V + \nabla P/\rho = \nu\nabla^2 V \tag{1}$$

$$\nabla\cdot V = 0 \tag{2}$$

in a bounded domain $\Omega$. In Eqs. (1) and (2), $V$ is the velocity vector, $P$ is the pressure, $\rho$ is density, and $\nu$ is kinematic viscosity.

To pose a physical problem completely, a set of boundary conditions must be given. The Navier-Stokes equations are of the second order for velocity and of the first order for pressure. Therefore, boundary conditions for velocity are either solely Dirichlet or Dirichlet plus Neumann boundary conditions. Pressure has Dirichlet boundary conditions on part of the boundary. Generally speaking, the boundary conditions for velocity are

$$V = V(x) \text{ on } \Gamma_1 \varepsilon \Gamma \equiv \partial\Omega \tag{3}$$

and

$$\frac{\partial V}{\partial n} = \frac{\partial V}{\partial n}(x) \text{ on } \Gamma_2 \varepsilon \Gamma \equiv \partial\Omega \tag{4}$$

Boundary conditions for pressure are

$$P = P(x) \text{ on } \Gamma_3 \varepsilon \Gamma \equiv \partial\Omega. \tag{5}$$

where $\Gamma_1 \cup \Gamma_2 \cup \Gamma_3 = \Gamma$.

On some boundaries both Dirichlet and Neumann boundary conditions for velocity exist when a viscous flow problem is solved. To implement boundary conditions in a numerical procedure, Dirichlet boundary conditions are implemented explicitly while Neumann boundary conditions are satisfied implicitly with the solutions. For example, along a solid wall, the no-penetration condition is implemented explicitly by the Dirichlet boundary condition. The Neumann boundary condition along walls is ignored, which is satisfied automatically by the continuity equation. However, in a numerical solution procedure of the incompressible Navier-Stokes equations, if both the no-penetration and the no-slip conditions are implemented explicitly for the momentum equations, numerical boundary conditions for pressure may also be needed on these boundaries. Otherwise, the matrix becomes ill-conditioned, resulting in spurious pressure solutions being obtained. On these boundaries where the physical boundary conditions for pressure are not known, a boundary equation for pressure can be implemented.[18] However, it is not very convenient to implement this equation in the resulting simultaneous linear algebra equations for the pressure nodes along solid wall boundaries. In the present work, the boundary condition switching procedure to implement both Dirichlet and Neumann boundary conditions for velocity is applied instead of implementing the pressure boundary equation. In this procedure, the pressure boundary equation is replaced by the Dirichlet boundary condition for velocity at the wall while the Neumann boundary condition for velocity at the wall is imposed for the related momentum equation. This approach is similar to that used when solving the stream function-vorticity formulation of the incompressible Navier-Stokes equations.[1] For different flow problems, boundaries where the boundary condition switching technique is applied are different. For the convection heat transfer in enclosures, detailed discussions will be shown in the following sections.

## Governing Equations and Boundary Conditions

### Square Cavity

The governing equations for incompressible laminar convection heat transfer with negligible viscous dissipation and no heat generation in a square cavity are given below:

$$\frac{\partial u}{\partial x} + \frac{\partial v}{\partial y} = 0 \tag{6}$$

$$u\frac{\partial u}{\partial x} + v\frac{\partial u}{\partial y} = -\frac{\partial P}{\partial x} + Pr\left[\frac{\partial^2 u}{\partial x^2} + \frac{\partial^2 u}{\partial y^2}\right] \tag{7}$$

$$u\frac{\partial v}{\partial x} + v\frac{\partial v}{\partial y} = -\frac{\partial P}{\partial y} + Pr\left[\frac{\partial^2 v}{\partial x^2} + \frac{\partial^2 v}{\partial y^2}\right] + RaPrT \tag{8}$$

$$u\frac{\partial T}{\partial x} + v\frac{\partial T}{\partial y} = \frac{\partial^2 T}{\partial x^2} + \frac{\partial^2 T}{\partial y^2} \tag{9}$$

where $u$ is nondimensional horizontal velocity, $v$ is nondimensional vertical velocity, $P$ is nondimensional pressure, and $T = (T' - T'_{\text{cold}})/(T'_{\text{hot}} - T'_{\text{cold}})$ is nondimensional temperature with $T'$ the local temperature. The length of square cavity on each side is $L$. $Pr = \nu/\alpha$ is the Prandtl number and $Ra = g\beta L^3\delta T/\alpha\nu$ is the Rayleigh number where $g$ is gravity, $\beta$ is the coefficient of thermal expansion, $\alpha$ is thermal diffusivity, and $\nu$ is kinematic viscosity.

The geometry of the square cavity and boundary conditions for convective heat transfer are shown in Fig. 1. Along the top and bottom, the walls are insulated and $\partial T/\partial y = 0$. On the hot side, the nondimensional temperature is equal to one. On the cold side, the temperature is equal to zero. Along the boundaries of the cavity, both velocity components are equal

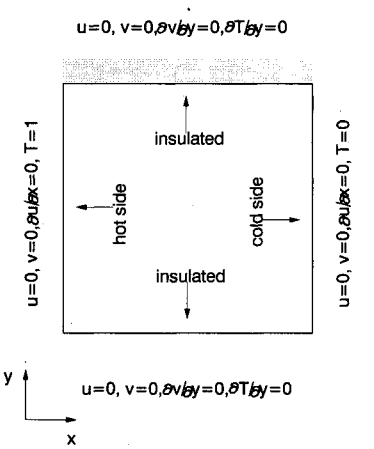


**Fig. 1 Boundary conditions for square cavity.**

to zero. These stationary flow conditions provide Dirichlet type boundary conditions. Neumann boundary conditions are obtained from continuity requirement along wall boundaries. Neumann boundary conditions require that the normal derivative of the normal component of velocity at wall boundaries is zero. Pressure boundary conditions are not required in this problem because pressure is not known in advance along wall boundaries.

**Vertical Annulus**

The governing equations for incompressible laminar heat convection flows are the continuity equation, the momentum equations, and the energy equation. The nondimensional forms are given below:

$$\frac{\partial v_r}{\partial r} + \frac{\partial v_z}{\partial z} + \frac{v_r}{r} = 0 \tag{10}$$

$$v_r \frac{\partial v_r}{\partial r} + v_z \frac{\partial v_r}{\partial z} = -\frac{\partial P}{\partial r} + Pr\left[\frac{\partial^2 v_r}{\partial r^2} + \frac{1}{r}\frac{\partial v_r}{\partial r} + \frac{\partial^2 v_r}{\partial z^2} - \frac{v_r}{r^2}\right] \tag{11}$$

$$v_r \frac{\partial v_z}{\partial r} + v_z \frac{\partial v_z}{\partial z} = -\frac{\partial P}{\partial z} + Pr\left[\frac{\partial^2 v_z}{\partial r^2} + \frac{1}{r}\frac{\partial v_z}{\partial r} + \frac{\partial^2 v_z}{\partial z^2}\right] + Ra^* PrT \tag{12}$$

$$v_r \frac{\partial T}{\partial r} + v_z \frac{\partial T}{\partial z} = \frac{\partial^2 T}{\partial r^2} + \frac{1}{r}\frac{\partial T}{\partial r} + \frac{\partial^2 T}{\partial z^2} \tag{13}$$

The annulus width is $L = r_o - r_i$ with $r_o$ the radius of the outer cylinder and $r_i$ the radius of the inner cylinder. The nondimensional radius of the inner and outer cylinder are respectively $R_i = r_i/L = 1/(\gamma - 1)$ and $R_o = r_o/L = \gamma/(\gamma - 1)$ where $\gamma = r_o/r_i$ is the diameter ratio. The dimensionless vertical length is $A = z_{top}/L$, the aspect ratio. The Rayleigh number is defined by $Ra^* = g\beta L^3(qL/k)/\alpha\nu$ where $q$ is the constant heat flux at the inner wall and $k$ is the thermal conductivity of the fluid.

The nondimensional variables are defined by

$$v_r = \frac{v_r' L}{\alpha}, \quad v_z = \frac{v_z' L}{\alpha}, \quad T = \frac{(T' - T_o')}{(qL/k)}, \quad P = \frac{L^2 P'}{\alpha^2 \rho} \tag{14}$$

where $v_r'$ is the dimensional radial velocity, $v_z'$ is the dimensional vertical velocity, $T'$ is the dimensional temperature, $T_o'$ is the temperature on the outer cylinder, $\rho$ is the density, and $P'$ is the dimensional pressure.

The geometry and boundary conditions for convective heat transfer in annuli are shown in Fig. 2. On the top and bottom of the annulus, it is insulated and, thus, the boundary condition for temperature is $\partial T/\partial z = 0$. On the outer cylinder, the nondimensional temperature value is zero by definition. On the inner cylinder, the gradient of the temperature is a constant because of the constant heat flux on the wall which requires $|\nabla T| = -1$ by the definition of the nondimensional temperature. The radial derivative of the temperature is $\partial T/\partial r = -\cos\alpha$. The velocity boundary conditions are similar to those of the square cavity. Dirichlet boundary conditions for velocity components are the no-slip and no-penetration conditions that require zero velocity on wall boundaries. Neumann boundary conditions are given by the continuity requirement. Along wall boundaries, the normal derivative of the normal component of the velocity is zero. The pressure boundary condition in this case is not required.

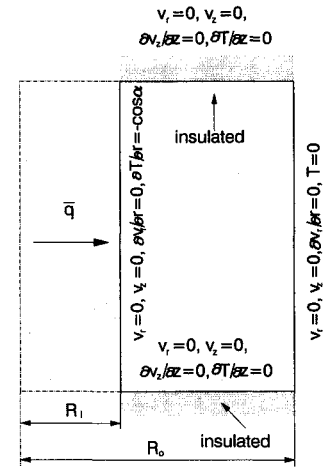


**Fig. 2 Boundary conditions for annulus.**

## Finite Element Formulation

It is well known that to solve the primitive variable form of the Navier-Stokes equations with the finite element method, special element or mixed interpolation should be used. Otherwise, oscillations in the pressure solutions will develop. With the boundary condition switching method, equal order interpolation can be used and solutions for pressure are smooth. Therefore, a simple element such as the bilinear element can be employed for every variable involved.

**Square Cavity**

In the finite element method, the weighted residual formulation is used to obtain the discretized simultaneous equations. Thus, the weak forms of Eqs. (6–9) are

$$\iint_\Omega W\left(\frac{\partial u}{\partial x} + \frac{\partial v}{\partial y}\right) dx dy = 0 \tag{15}$$

$$\iint_\Omega W\left[u\frac{\partial u}{\partial x} + v\frac{\partial u}{\partial y} + \frac{\partial P}{\partial x} - Pr\left(\frac{\partial^2 u}{\partial x^2} + \frac{\partial^2 u}{\partial y^2}\right)\right] dx dy = 0 \tag{16}$$

$$\iint_\Omega W\left[u\frac{\partial v}{\partial x} + v\frac{\partial v}{\partial y} + \frac{\partial P}{\partial y} - Pr\left(\frac{\partial^2 v}{\partial x^2} + \frac{\partial^2 v}{\partial y^2}\right) - RaPrT\right] dx dy = 0 \tag{17}$$

$$\iint_\Omega W\left(u\frac{\partial T}{\partial x} + v\frac{\partial T}{\partial y} - \frac{\partial^2 T}{\partial x^2} + \frac{\partial^2 T}{\partial y^2}\right) dx dy = 0 \tag{18}$$

where $W$ is the weighting function. In Eqs. (16–18), applying Green's theorem to the second-order term and choosing the weighting function $W$ to be the shape function $N$, we have

$$\iint_\Omega \left[N\left(u\frac{\partial u}{\partial x} + v\frac{\partial u}{\partial y} + \frac{\partial P}{\partial x}\right) + Pr\left(\frac{\partial N}{\partial x}\frac{\partial u}{\partial x} + \frac{\partial N}{\partial y}\frac{\partial u}{\partial y}\right)\right] dx dy = \int_\Gamma PrN\frac{\partial u}{\partial n} dS \tag{19}$$

$$\iint_\Omega \left[N\left(u\frac{\partial v}{\partial x} + v\frac{\partial v}{\partial y} + \frac{\partial P}{\partial y} - RaPrT\right) + Pr\left(\frac{\partial N}{\partial x}\frac{\partial v}{\partial x} + \frac{\partial N}{\partial y}\frac{\partial v}{\partial y}\right)\right] dx dy = \int_\Gamma PrN\frac{\partial v}{\partial n} dS \tag{20}$$

$$\iint_\Omega \left[ N\left(u\frac{\partial T}{\partial x} + v\frac{\partial T}{\partial y}\right) + \frac{\partial N}{\partial x}\frac{\partial T}{\partial x} + \frac{\partial N}{\partial y}\frac{\partial T}{\partial y}\right] dxdy = \int_\Gamma N\frac{\partial T}{\partial n}\,dS \tag{21}$$

The Neumann boundary conditions for the thermal component of velocity at the walls are satisfied automatically because the boundary integrals for the velocity normal components vanish. Thus, the no-penetration condition can be used to replace the continuity equation along that boundary for pressure representation. Therefore, both Dirichlet and Neumann boundary conditions for velocity are satisfied and no extra boundary conditions for pressure are required. The boundary condition for the tangential component of the velocity along wall boundaries is implemented by the given Dirichlet condition. The boundary conditions for temperature on the top and bottom of the cavity are satisfied because the boundary integral is equal to zero. On the hot and cold sides of the cavity, the given temperature values are implemented.

Bilinear elements are used in this work and the appropriate piecewise polynomial basis functions for velocity components $u$, $v$, pressure $P$, and temperature $T$ are

$$u = \sum_{k=1}^{4} N_k u_k \tag{22}$$

$$v = \sum_{k=1}^{4} N_k v_k \tag{23}$$

$$P = \sum_{k=1}^{4} N_k P_k \tag{24}$$

$$T = \sum_{k=1}^{4} N_k T_k \tag{25}$$

The discretized simultaneous equations for velocity components and pressure are built up using the local stiffness matrix

$$M = \begin{bmatrix} K_{u,u} & 0 & K_{u,p} \\ 0 & K_{v,v} & K_{v,p} \\ K_{p,u} & K_{p,v} & 0 \end{bmatrix} \tag{26}$$

where

$$K_{u,u} = \iint \left(NV\cdot\nabla u + Pr\nabla N\cdot\nabla u\right) dxdy$$

$$K_{u,p} = \iint N\frac{\partial P}{\partial_x}\,dxdy$$

$$K_{v,v} = \iint \left(NV\cdot\nabla v + Pr\nabla N\cdot\nabla v\right) dxdy$$

$$K_{v,p} = \iint N\frac{\partial P}{\partial y}\,dxdy$$

$$K_{p,u} = \iint N\frac{\partial u}{\partial_x}\,dxdy, \quad K_{p,v} = \iint N\frac{\partial v}{\partial y}\,dxdy$$

and the energy equation is solved after velocity components are obtained.

**Vertical Annuli**

For convection heat transfer in annuli, the integration weak forms of Eqs. (10–13) are

$$\iint_\Omega W\left(\frac{\partial v_r}{\partial r} + \frac{\partial v_z}{\partial z} + \frac{v_r}{r}\right) drdz = 0 \tag{27}$$

$$\iint_\Omega W\left[v_r\frac{\partial v_r}{\partial r} + v_z\frac{\partial v_r}{\partial z} + \frac{\partial P}{\partial r} - Pr\left(\frac{\partial^2 v_r}{\partial r^2} + \frac{1}{r}\frac{\partial v_r}{\partial r} + \frac{\partial^2 v_r}{\partial z^2} - \frac{v_r}{r^2}\right)\right] drdz = 0 \tag{28}$$

$$\iint_\Omega W\left[v_r\frac{\partial v_z}{\partial r} + v_z\frac{\partial v_z}{\partial z} + \frac{\partial P}{\partial z} - Ra^*PrT - Pr\left(\frac{\partial^2 v_z}{\partial r^2} + \frac{1}{r}\frac{\partial v_z}{\partial r} + \frac{\partial^2 v_z}{\partial z^2}\right)\right] drdz = 0 \tag{29}$$

$$\iint_\Omega W\left[v_r\frac{\partial T}{\partial r} + v_z\frac{\partial T}{\partial z} - \left(\frac{\partial^2 T}{r^2} + \frac{1}{r}\frac{\partial T}{\partial r} + \frac{\partial^2 T}{\partial z^2}\right)\right] drdz = 0 \tag{30}$$

In Eqs. (28–30), applying Green's theorem to the second order term and choosing the weighting function $W$ to be the shape function $N$, we have

$$\iint_\Omega \left[N\left(v_r\frac{\partial v_r}{\partial r} + v_z\frac{\partial v_r}{\partial z} + \frac{\partial P}{\partial r}\right) + Pr\left[\frac{\partial N}{\partial r}\frac{\partial v_r}{\partial r} + \frac{\partial N}{\partial z}\frac{\partial v_r}{\partial z} + N\left(-\frac{1}{r}\frac{\partial v_r}{\partial r} + \frac{v_r}{r^2}\right)\right]\right] drdz = 0 \tag{31}$$

$$\iint_\Omega \left[N\left(v_r\frac{\partial v_z}{\partial r} + v_z\frac{\partial v_z}{\partial z} + \frac{\partial P}{\partial z} - Ra^*PrT\right) + Pr\left[\frac{\partial N}{\partial r}\frac{\partial v_z}{\partial r} + \frac{\partial N}{\partial z} - N\frac{1}{r}\frac{\partial v_z}{\partial r}\right]\right] drdz = 0 \tag{32}$$

$$\iint_\Omega \left[N\left(v_r\frac{\partial T}{\partial r} + v_z\frac{\partial T}{\partial z} - \frac{1}{r}\frac{\partial T}{\partial r}\right) + \frac{\partial N}{\partial r}\frac{\partial T}{\partial r} + \frac{\partial N}{\partial z}\frac{\partial T}{\partial z}\right] drdz = 0 \tag{33}$$

The implementation procedure for boundary conditions in convection heat transfer in annuli is the same as in the case of a square cavity. The normal derivative of the normal velocity component is zero and the boundary integrals vanish. The no-penetration condition can be used to substitute the continuity equation along the boundary for the pressure. In this way, both Dirichlet and Neumann boundary conditions for velocity are implemented with the continuity equation satisfied. The boundary conditions for pressure are not required. On the top and bottom of the annuli, the normal derivative of the temperature is zero. This condition is satisfied because the boundary integral is equal to zero. On the cold side of the cavity, the given temperature value is implemented. On the hot side, the normal derivative of the temperature is given by the constant heat flux condition. This condition is satisfied by implementing the boundary integral along the boundary.

Bilinear elements are also used for the heat transfer problem in the vertical annulus. The appropriate piecewise polynomial basis functions for velocity components $u$, $v$, pressure $P$, and temperature $T$ are the same as given by Eqs. (22–25). The discretized simultaneous equations for velocity components and pressure are assembled using the local stiffness matrix given by Eq. (26) in which $u$ is replaced by the radial component of velocity $v_r$ and $v$ is replaced by the vertical component of the velocity $v_z$. The integrals of the velocity components and the pressure for the vertical annulus are

$$K_{v_r,v_r} = \iint \left[N\left(v_r\frac{\partial v_r}{\partial r} + v_z\frac{\partial v_r}{\partial z}\right) + Pr\left[\frac{\partial N}{\partial r}\frac{\partial v_r}{\partial r} + \frac{\partial N}{\partial z}\frac{\partial v_r}{\partial z} + N\left(-\frac{1}{r}\frac{\partial v_r}{\partial r} + \frac{v_r}{r^2}\right)\right]\right] drdz$$

$$K_{v_r,p} = \iint N \frac{\partial P}{\partial r}\, dr dz$$

$$K_{v_z,v_z} = \iint \left[ N \left( v_r \frac{\partial v_z}{\partial r} + v_z \frac{\partial v_z}{\partial z} \right) + Pr \left[ \frac{\partial N}{\partial r}\frac{\partial v_z}{\partial r} + \frac{\partial N}{\partial z}\frac{\partial v_z}{\partial z} - N\frac{1}{r}\frac{\partial v_z}{\partial r} \right] \right] dr dz$$

$$K_{v_z,p} = \iint N \frac{\partial P}{\partial z}\, dr dz$$

$$K_{p,v_r} = \iint N \left[ \frac{\partial v_r}{\partial r} + \frac{v_r}{r} \right] dr dz$$

$$K_{p,v_z} = \iint N \frac{\partial v_z}{\partial z}\, dr dz$$

The temperature term in Eq. (29) is used to build up the right-hand side of the simultaneous equations. The energy equation is solved separately after solutions of the velocity components are obtained.

The nonlinear equation systems for both the square cavity and the vertical annulus are solved iteratively using the Newton-Raphson method.

## Finite Difference Formulation

The difficulty in solving the Navier-Stokes equations with primitive variables is that if central difference formulations are used for the first order pressure terms, the pressure is decoupled across mesh points. This results in oscillations in the pressure solutions. To avoid this problem, either staggered grids or upwind differences are used. With the boundary condition switching scheme, the central difference formulation can be used. In this work, the second order central difference is applied to formulate the difference equations for grid points inside the domain.

### Square Cavity

For the convection heat transfer flow in a square cavity, the governing equations are given by Eqs. (6–9). The finite difference equations for each grid point $i, j$ are

$$\frac{\bar{\delta}_x u^n_{i,j}}{2\Delta x} + \frac{\bar{\delta}_y v^n_{i,j}}{2\Delta y} = 0 \tag{34}$$

$$u^{n-1}_{i,j}\frac{\bar{\delta}_x u^n_{i,j}}{2\Delta x} + v^{n-1}_{i,j}\frac{\bar{\delta}_y u^n_{i,j}}{2\Delta y} + \frac{\bar{\delta}_x P^n_{i,j}}{2\Delta x} - Pr\left[ \frac{\delta^2_x u^n_{i,j}}{\Delta x^2} + \frac{\delta^2_y u^n_{i,j}}{\Delta y^2} \right] = 0 \tag{35}$$

$$u^{n-1}_{i,j}\frac{\bar{\delta}_x v^n_{i,j}}{2\Delta x} + v^{n-1}_{i,j}\frac{\bar{\delta}_y v^n_{i,j}}{2\Delta y} + \frac{\bar{\delta}_y P^n_{i,j}}{2\Delta y} - Pr\left[ \frac{\delta^2_x v^n_{i,j}}{\Delta x^2} + \frac{\delta^2_y v^n_{i,j}}{\Delta y^2} \right] = RaPrT^{n-1}_{i,j} \tag{36}$$

$$u^n_{i,j}\frac{\bar{\delta}_x T^n_{i,j}}{2\Delta x} + v^n_{i,j}\frac{\bar{\delta}_y T^n_{i,j}}{2\Delta y} - \left[ \frac{\delta^2_x T^n_{i,j}}{\Delta x^2} + \frac{\delta^2_y T^n_{i,j}}{\Delta y^2} \right] = 0 \tag{37}$$

where $\Delta x$ and $\Delta y$ are the grid increments and

$$\bar{\delta}_x q_{i,j} = q_{i+1,j} - q_{i-1,j} \tag{38}$$

$$\bar{\delta}_y q_{i,j} = q_{i,j+1} - q_{i,j-1} \tag{39}$$

$$\delta^2_x q_{i,j} = q_{i+1,j} - 2q_{i,j} + q_{i-1,j} \tag{40}$$

$$\delta^2_y q_{i,j} = q_{i,j+1} - 2q_{i,j} + q_{i,j-1} \tag{41}$$

where

$$q = \begin{Bmatrix} u \\ v \\ P \\ T \end{Bmatrix}$$

The Neumann boundary conditions for the normal component of velocity at the wall can be satisfied if we apply the finite difference equations for the momentum equations to grid points on the boundaries where both Dirichlet and Neumann boundary conditions exist. For instance, for the horizontal wall on the top of the cavity, we have $u = 0$, $v = 0$, and $\partial v/\partial y = 0$. Thus, Eq. (36) becomes

$$\frac{\Delta P^n_{i,j}}{\Delta y} + Pr\left[ \frac{2\Delta v^n_{i,j}}{\Delta y^2} \right] = RaPrT^{n-1}_{i,j} \tag{42}$$

The Dirichlet boundary condition $v = 0$ is switched to substitute the continuity equation representing the pressure. In this way, both Dirichlet and Neumann boundary conditions are implemented with continuity equation satisfied. With boundary condition switching staggered grids are not necessary.

### Vertical Annulus

For the convection heat transfer flow in a vertical annulus, the governing equations are given by Eqs. (10–13). The finite difference equations for grid point $(i, j)$ are

$$\frac{\bar{\delta}_r v^n_{ri,j}}{2\Delta r} + \frac{\bar{\delta}_z v^n_{zi,j}}{2\Delta z} + \frac{v^n_{ri,j}}{r_{i,j}} = 0 \tag{43}$$

$$v^{n-1}_{ri,j}\frac{\bar{\delta}_r v^n_{ri,j}}{2\Delta r} + v^{n-1}_{zi,j}\frac{\bar{\delta}_z v^n_{ri,j}}{2\Delta z} + \frac{\bar{\delta}_r P^n_{i,j}}{2\Delta r} - Pr\left[ \frac{\delta^2_r v^n_{ri,j}}{\Delta r^2} + \frac{\delta^2_z v^n_{ri,j}}{\Delta z^2} + \frac{1}{r_{i,j}}\frac{\bar{\delta}_r v^n_{ri,j}}{2\Delta r} - \frac{v^n_{ri,j}}{r^2_{i,j}} \right] = 0 \tag{44}$$

$$v^{n-1}_{ri,j}\frac{\bar{\delta}_r v^n_{zi,j}}{2\Delta r} + v^{n-1}_{zi,j}\frac{\bar{\delta}_z v^n_{zi,j}}{2\Delta z} + \frac{\bar{\delta}_z P^n_{i,j}}{2\Delta z} - Pr\left[ \frac{\delta^2_r v^n_{zi,j}}{\Delta r^2} + \frac{\delta^2_z v^n_{zi,j}}{\Delta z^2} + \frac{1}{r_{i,j}}\frac{\bar{\delta}_r v^n_{zi,j}}{2\Delta r} \right] = Ra^* PrT^{n-1}_{i,j} \tag{45}$$

$$v^n_{ri,j}\frac{\bar{\delta}_r T^n_{i,j}}{2\Delta r} + v^n_{zi,j}\frac{\bar{\delta}_z T^n_{i,j}}{2\Delta z} - \left[ \frac{\delta^2_r T^n_{i,j}}{\Delta r^2} + \frac{\delta^2_z T^n_{i,j}}{\Delta z^2} + \frac{1}{r_{i,j}}\frac{\bar{\delta}_r T^n_{i,j}}{2\Delta r} \right] = 0 \tag{46}$$

where $\Delta r$ and $\Delta z$ are the grid increment.

By using the Neumann boundary conditions for the normal component of velocity at the wall, the finite difference equations for the momentum equations at grid points on the boundaries become

$$\frac{\Delta P^n_{i,j}}{\Delta z} \pm Pr\left[ \frac{2\Delta v^n_{zi,j}}{\Delta z^2} \right] = Ra^* PrT^{n-1}_{i,j} \tag{47}$$

on the top and bottom of the vertical annulus and

$$\frac{\Delta P^n_{i,j}}{\Delta r} \pm Pr\left[ \frac{2\Delta v^n_{ri,j}}{\Delta r^2} \right] = 0 \tag{48}$$

on the outer and inner cylinder. The Dirichlet boundary conditions for the momentum equation of the normal component of the velocity are switched to replace the continuity equation representing the pressure. In this way, both Dirichlet and Neumann boundary conditions are implemented with the continuity equation satisfied.

**Table 1 Solutions for square cavity**

| | This work | | | de Vahl Davis[16] | | | | Hortmann et al.[17] | | |
|---|---|---|---|---|---|---|---|---|---|---|
| *Ra* | *Nu* | $Nu_{max}$ *y* | $Nu_{min}$ *y* | *Nu* | $Nu_b$ | $Nu_{max}$ *y* | $Nu_{min}$ *y* | *Nu* | $Nu_b$ | $Nu_{max}$ *y* |
| $10^3$ | 1.119 | 1.507<br>0.075 | 0.694<br>1.0 | 1.116 | 1.117 | 1.501<br>0.087 | 0.694 | | | |
| $10^4$ | 2.245 | 3.554<br>0.15 | 0.587<br>1.0 | 2.242 | 2.238 | 3.545<br>0.149 | 0.592<br>1.0 | 2.244 | 2.245 | 3.537 |
| $10^5$ | 4.589 | 8.030<br>0.075 | 0.724<br>1.0 | 4.564 | 4.509 | 7.905<br>0.095 | 0.755<br>1.0 | 4.617 | 4.523 | 8.151 |
| $10^6$ | 9.170 | 19.97<br>0.05 | 0.834<br>1.0 | 9.270 | 8.817 | 17.95<br>0.068 | 1.015<br>0.984 | 9.422 | 8.835 | 20.90 |

**Table 2 Solutions for annuli**

| | | | *Nu* | |
|---|---|---|---|---|
| *Ra** | *A* | *K* | This work | Bhushan et al.[3] |
| $10^6$ | 38.00 | 1.23 | 4.01 | 3.97 |
| $10^7$ | 38.00 | 1.23 | 6.98 | 6.96 |
| $10^6$ | 52.82 | 2.77 | 4.77 | 5.04 |

## Results and Discussion

The first test problem for natural heat convection in enclosures is the incompressible laminar flow in a square cavity with the top and the bottom insulated and constant temperatures on hot and cold sides. For this problem, benchmark solutions can be found (de Vahl Davis[16] and Hortmann et al.[17]). Numerical solutions for this problem can be compared with the benchmark solutions to verify the scheme. The fluid is assumed to be a Boussinesq's fluid with the Prandtl number equal to 0.71. The cavity side length is taken to be unity. The geometry and boundary conditions are shown in Fig. 1. Velocity components are zero along the boundaries. The normal derivatives of the normal velocity components are also zero along the boundaries. The Neumann boundary condition is implemented in the momentum equation for the normal velocity component; the Dirichlet boundary condition for the normal velocity component is switched to replace the continuity equation for pressure representation. On the top and bottom of the cavity, the walls are insulated; thus, the normal derivative of the temperature is zero. Nondimensional temperature at the cold and hot walls are set to zero and unity respectively.

In this example, a grid system with 41 × 41 nodes is employed. Both the finite element method and the finite difference method are implemented on the same grid. Numerical results obtained by both methods are close to each other. The difference between them are within 0.5%. Numerical results are obtained by Rayleigh numbers of $10^3$, $10^4$, $10^5$, and $10^6$. Isotherms of the temperature fields are shown in Fig. 3. Isothermal values are equally divided when plotting the figures. In Fig. 4, isobars are presented. The isovalues of the pressure are also equally divided when plotting the figures. The pressure solutions are smooth and there is no oscillation found. Thus, the pressure values do not need to be filtered. The numerical solutions obtained by the boundary condition switching method are compared with the benchmark solutions in Table 1. The results of this work are very close to the results obtained by other methods[16,17] on a 41 × 41 grid. The differences between the results obtained on the 41 × 41 grid in this work and the benchmark solutions are within 1% for Rayleigh numbers less than $10^5$. For Rayleigh number of $10^6$, the error is less than 4%.

The second problem solved with the solution procedure developed in this work is natural convection within an annulus with a range of aspect ratios from unity to 53. The definition of the flowfield geometry and boundary conditions are shown in Fig. 2 where $R_i$ is the inner cylinder radius and $R_o$ is the outer cylinder radius of the annulus. The diameter ratio is defined as $K = R_o/R_i$. The nondimensional vertical size is

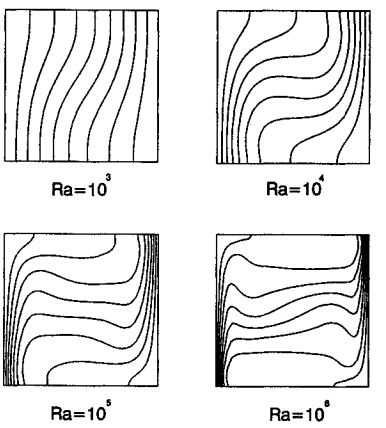


**Fig. 3 Isotherms for square cavity.**

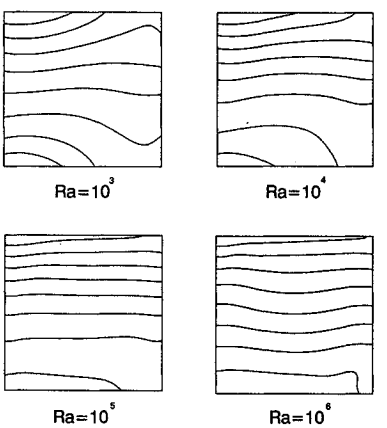


**Fig. 4 Iso-bars for square cavity.**

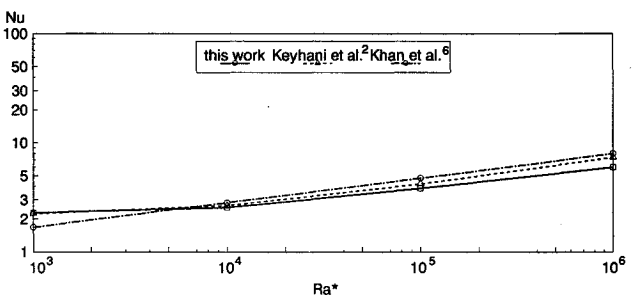


**Fig. 5 Nu vs *Ra**, $A = 27.6$, $K = 4.33$.**

the aspect ratio $A$. The actual height of the annulus is determined by $Z = A(R_o - R_i)$. The outer cylinder is kept at a nondimensional temperature of zero. On the inner surface of the annulus, a constant heat flux is supplied. On the top and bottom, the annulus is insulated. The Dirichlet boundary conditions on all wall boundaries are the velocity boundary conditions, which require that both components of the velocity are zeros. The Neumann boundary condition is given by the continuity equation, which assumes that the normal derivative of the normal velocity component be zero. For the normal

**Table 3 Comparison between numerical results**

| | | | This work | | | Khan et al.[6] | | |
|---|---|---|---|---|---|---|---|---|
| $Ra^*$ | $A$ | $K$ | $T_{max}/T_a$ | $T_{min}/T_a$ | $Nu$ | $T_{max}/T_a$ | $T_{min}/T_a$ | $Nu$ |
| $5 \times 10^4$ | 1 | 2 | 1.450 | 0.809 | 3.692 | 1.475 | 0.791 | 3.770 |
| | | 5 | 1.411 | 0.835 | 4.900 | 1.442 | 0.856 | 4.999 |
| | | 10 | 1.358 | 0.856 | 6.137 | 1.416 | 0.881 | 6.053 |
| | | 15 | 1.320 | 0.868 | 7.328 | 1.377 | 0.891 | 6.777 |
| $10^6$ | 1 | 2 | 1.655 | 0.758 | 7.493 | 1.943 | 0.682 | 7.398 |
| | | 5 | 1.606 | 0.795 | 9.213 | 1.769 | 0.830 | 9.809 |
| | | 10 | 1.547 | 0.785 | 10.95 | 1.762 | 0.881 | 11.88 |
| | | 15 | 1.503 | 0.838 | 12.40 | 1.603 | 0.863 | 13.30 |
| $6.25 \times 10^4$ | 1 | 2 | 1.465 | 0.808 | 3.890 | 1.535 | 0.798 | 3.965 |
| | 2 | | 1.656 | 0.748 | 3.859 | 1.686 | 0.745 | 3.830 |
| | 5 | | 1.755 | 0.667 | 3.536 | 1.688 | 0.624 | 3.658 |

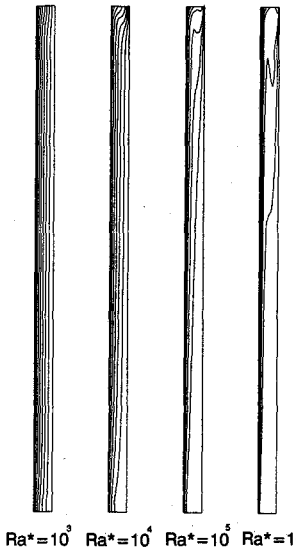


**Fig. 6 Isotherms, $A = 27.6$, $K = 4.33$.**

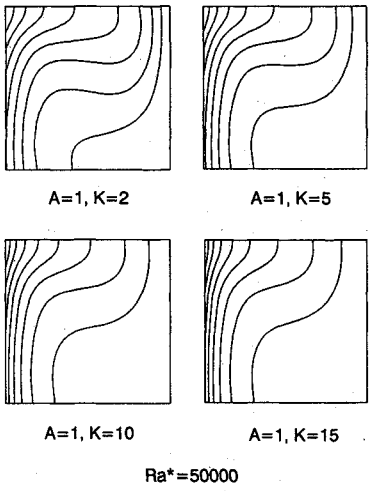


**Fig. 7 Isotherms, $Ra^* = 5 \times 10^4$.**

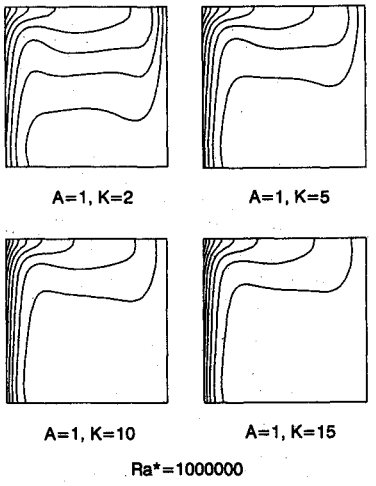


**Fig. 8 Isotherms, $Ra^* = 10^6$.**

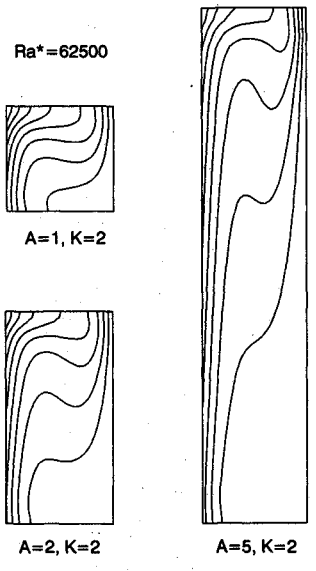


**Fig. 9 Isotherms, $Ra^* = 6.25 \times 10^4$.**

velocity component, the Neumann boundary condition is implemented in the momentum equation; the velocity boundary condition is switched to substitute the continuity equation for pressure representation. In the boundary condition switching solution procedure, both Dirichlet and Neumann boundary conditions are explicitly implemented with the continuity equation satisfied. The constant heat flux condition is implemented by searching the temperature gradient on the inner cylinder. In Khan and Kumar's work,[6] this condition is imposed by $\partial T/\partial r = -1$, which is incorrect because the temperature on the inner cylinder is not a constant, thus, the temperature gradient is not in the normal direction of the inner cylinder. The normal derivative of the temperature on the inner cylinder should be equal to $\cos\alpha$ where $\alpha$ is the direction angle between the temperature gradient and the normal vector of the inner cylinder. This condition is implemented in the present work by $\partial T^n/\partial r = \sqrt{1 - (\partial T^{n-1}/\partial z)^2}$.

Solutions are obtained on a grid $41 \times 41$ for low aspect ratio $A \leq 5$, $41 \times 81$ for $5 < A \leq 15$ and $41 \times 161$ for $A > 15$. Both finite element and finite difference methods are applied on the same grid. The numerical solutions with each method are very close to each other. In Fig. 5, the compar-

isons among the results obtained in this work, experimental data and other numerical results are shown for Rayleigh number from $10^3$ to $10^6$, as aspect ratio of 27.6 and a diameter ratio of 4.33. For low Rayleigh numbers, the results in this work agree well with the experimental data. For high Rayleigh numbers, our results predict lower heat transfer rate. The results by Ref. 6 are calculated by the correlation provided by the authors because no specific values are presented in their paper. In Fig. 6, the isothermal lines of the temperature field are shown. The isoline values are equally divided on the figures. The numerical computations are also performed for natural convection at high Rayleigh numbers and aspect ratios. In Table 2, comparisons among the present results and the experimental data are shown. For $A = 38$ and $K = 1.23$, the present results agree very well with experimental data. For $A = 52.82$ and $K = 2.77$, the difference between our results and the experimental data is about 5%.

In Fig. 7, isotherms are presented for Rayleigh number of $5 \times 10^4$, aspect ratio $A = 1$, and diameter ratio $K$ from 2 to 15. As shown, in Fig. 7, for the same Rayleigh number and the same aspect ratio, the temperature changes more rapidly near the inner cylinder as diameter ratio increases. This indicates that with the same amount of heat flux at the inner cylinder, higher heat transfer rates can be obtained when the diameter ratio increases. The physical explanation is that when the diameter ratio increases, the outer cylinder area increases with the same amount of heat supply on the inner cylinder and, therefore, the heat transfer inside the annulus is enhanced. The Nusselt numbers calculated for different diameter ratios are shown in Table 3. In Fig. 8, isothermal fields for Rayleigh number of $10^6$, aspect ratio $A = 1$ and the same diameter ratios in the above case are shown. Isotherms are located closer to the inner cylinder for higher Rayleigh number. This indicates that with the same geometry, when more heat is supplied on the inner cylinder, the heat transfer rate increases. The heat transfer rates calculated for Rayleigh number of $10^6$ with the same geometry are shown in Table 3. In Fig. 9, isothermals are shown for the natural convection case with Rayleigh number of $6.25 \times 10^4$, diameter ratio $K = 2$, and aspect ratio of 1, 2, and 5. The effect of the aspect ratio to the heat transfer rate is not as significant as that for the diameter. The isoline patterns look similar to each other for different aspect ratios. The temperature difference between the maximum and minimum temperatures on the inner cylinder is bigger for higher aspect ratio. The nonevenly distributed temperature on the inner cylinder reduces the overall heat transfer slightly. For example, the Nusselt number for aspect ratio of 5 is 2% lower than the one for aspect ratio of 1. The Nusselt numbers calculated for this case are also shown in Table 3.

## Conclusions

This work shows that the boundary condition switching method for solutions of the stream function-vorticity equations can be applied to solve the Navier-Stokes equations with primitive variables. When the boundary condition switching procedure is used with the finite element technique, equal order interpolation can be used for both velocity and pressure. When the boundary condition switching procedure is applied with the finite difference method, nonstaggered grids can be used with velocity and pressure defined on the same grid system. Equal order interpolation in the finite element method and use of a nonstaggered grid in finite difference method require less calculations to build up the local matrices and are easy to program.

The difficulty encountered when solving pressure in the incompressible Navier-Stokes equations with primitive variables can be overcome. In this work, numerical pressure boundary equations and upwind finite element formulations for pressure are not needed. With the boundary condition switching method, there are no pressure oscillations in the numerical solutions. Pressure smoothing and filtering procedures are not needed. Natural convection heat transfer in enclosures is likewise solved by the boundary condition switching method. Good agreement among the numerical results obtained in this work and benchmark solutions in the literature are obtained for natural convection in a square cavity. For natural convection flows in annuli, the numerical results agree fairly well with experimental data and published numerical solutions.

## References

[1]Sheriff, N., "Experimental Investigation of Natural Convection in Single and Multiple Vertical Annuli with High Pressure Carbon Dioxide," *Proceedings of the Third International Heat Transfer Conference,* Chicago, IL, Vol. 2, 1966, pp. 132–138.

[2]Keyhani, M., Kulacki, F. A., and Christensen, R. N., "Free Convection in a Vertical Annulus with Constant Heat Flux at the Inner Wall," *Journal of Heat Transfer,* Vol. 105, No. 3, 1983, pp. 454–459.

[3]Bhushan, R., Keyhani, M., Christensen, R. N., and Kulacki, R. A., "Correlation Equations for Free Convection in a Vertical Annulus with Constant Heat Flux on the Inner Wall," *Journal of Heat Transfer,* Vol. 105, No. 4, 1983, pp. 910–912.

[4]De Vahl Davis, G., and Thomas, R. W., "Natural Convection between Concentric Vertical Cylinders," *Physics of Fluids,* Supplement II, 1969, pp. 198–207.

[5]Thomas, R. W., and de Vahl Davis, G., "Natural Convection in Annular and Rectangular Cavities—A Numerical Study," *Proceedings of the Fourth International Heat Transfer Conference,* Paris, Vol. 4, Paper N.C. 2.4, 1970.

[6]Khan, J. A., and Kumar, R., "Natural Convection in Vertical Annuli: A Numerical Study for Constant Heat Flux on the Inner Wall," *Journal of Heat Transfer,* Vol. 111, No. 4, 1989, pp. 909–915.

[7]Peeters, M. F., Habashi, W. G., and Dueck, E. G., "Finite Element Stream Function-Vorticity Solutions of the Incompressible Navier-Stokes Equations," *International Journal for Numerical Methods in Fluids,* Vol. 7, No. 1, 1987, pp. 17–27.

[8]Cheng, R. T., "Numerical Solution of the Navier-Stokes equations by the Finite Element Method," *Physics of Fluids,* Vol. 15, No. 12, 1972, pp. 2098–2105.

[9]Baker, A. J., "Finite Element Solution Algorithm for Viscous Incompressible Fluid Dynamics," *International Journal for Numerical Methods in Engineering,* Vol. 6, No. 1, 1973, pp. 89–101.

[10]Campion-Renson, A., and Crochet, M. J., "On the Stream Function Vorticity Finite Element Solutions of Navier-Stokes Equations," *International Journal for Numerical Methods in Engineering,* Vol. 12, No. 12, 1978, pp. 1809–1818.

[11]Dhatt, G., Fomo, B. K., and Bourque, C. A., "A $\psi$–$\omega$ Finite Element Formulation for the Navier-Stokes Equations," *International Journal for Numerical Methods in Engineering,* Vol. 17, No. 2, 1981, pp. 199–212.

[12]Fang, Z., and Saber, A. J., "Marching Control Volume Finite Element Calculation for Developing Entrance Flow," *AIAA Journal,* Vol. 25, No. 2, 1987, pp. 346–348.

[13]Habashi, W., Peeters, M., Guevremont, G., and Hafes, M., "Finite Element Solutions of the Compressible Navier-Stokes Equations," *AIAA Journal,* Vol. 25, No. 7, 1987, pp. 944–948.

[14]Sani, R. L., Gresho, P. M., Lee, R. L., and Griffiths, D. F., "The Cause and Cure (?) of the Spurious Pressure Generated by Certain FEM Solutions of the Incompressible Navier-Stokes Equations: Part 1," *International Journal for Numerical Methods in Fluids,* Vol. 1, No. 1, 1981, pp. 17–43.

[15]Strikwerda, J. C., "Finite Difference Methods for the Stokes and Navier-Stokes Equations," *Society of Industrial and Applied Mechanics Journal on Scientific and Statistical Computing,* Vol. 5, No. 1, 1984, pp. 56–68.

[16]De Vahl Davis, G., "Natural Convection of Air in a Square Cavity: a Bench Mark Numerical Solution," *International Journal for Numerical Methods in Fluids,* Vol. 3, No. 3, 1983, pp. 249–264.

[17]Hortmann, M., Peric, M., and Scheuerer, G., "Finite Volume Multigrid Prediction of Laminar Natural Convection: Bench-Mark Solutions," *International Journal for Numerical Methods in Fluids,* Vol. 11, No. 2, 1990, pp.189–207.

[18]Fang, Z., Saber, A. J., "Solutions of the Incompressible Navier-Stokes Equations Using a Weighted Residual Method," *Proceedings of the Sixth International Conference on Laminar and Turbulent Flow,* Swansea, Wales, UK, July 1989, pp. 11–15.